Optimization of the Geometry of Monitoring Devices for Contaminant Detection in Cement-Bentonite Cutoff Walls

Optimization of the geometry of monitoring devices for contaminant detection in cement-bentonite cutoff walls

Giulia Scelsi[1], Gabriele Della Vecchia[1,*], Claudio di Prisco[1], Guido Musso[2] and Gianluigi Sanetti[3]

[1] Department of Civil and Environmental Engineering (DICA), Politecnico di Milano
piazza Leonardo da Vinci 32, 20133, Milano (Italy)
gabriele.dellavecchia@polimi.it

[2] Department of Structural, Geotechnical and Building Engineering (DISEG), Politecnico di Torino
Corso Duca degli Abruzzi, 24 - 10129 Torino (Italy)

[3] Ministero dello Sviluppo Economico (MISE), DGS UNMIG
Via Molise, 2, 00187 Roma (Italy)

Abstract Cutoff walls represent an interesting solution for the containment of the pollution of superficial groundwater. For polluted sites, the purpose of a cement-bentonite cutoff wall is to minimize contaminant transport and the primary design requirement for such materials is the low hydraulic conductivity. Despite these barriers are often cast in place as provisional tools, recently their wide use imparted the need for a better understanding of cement-bentonite walls also in the long-term. This certainly implies not only the need to study the time evolution of the cement-bentonite hydro-mechanical properties in a contaminated environment, but also the necessity of a continuous monitoring of the efficiency of the system. To this aim, the use of dedicated devices cast in place inside the wall when the mixture is still fluid proved to be particularly suitable to intercept and analyse the fluids flowing through the barrier. In this paper, the results of a numerical study are presented, with the goal of suggesting criteria about the optimum spacing and geometry of these devices.
Keywords: cutoff walls, cement-bentonite, contaminants, monitoring

1 Introduction

Containment is a widely used pollution control strategy, involving 'putting a box' around the contaminated ground. Slurry trenching is the most widely used form of trench barrier, and involves excavating a trench through a dense slurry and then backfilling the trench. Slurry trench cutoff walls were originally developed to control ground water flow beneath dams and levees, and for temporary excavations below the ground water table (Soga et al., 2013). With time, society became aware of subsurface contamination from industrial and storage activities and slurry trench cutoff walls proved to be a reliable technology to limit the underground circulation of pollutants. To achieve this goal, a backfill hydraulic conductivity lower than 10^{-9} m/s is specified in slurry wall design (ICE, 1999). Other requirements for slurry mixtures are a sufficient shear strength and ductility, as well as chemical compatibility with the permeating fluid. Among the different materials used for such barriers, a widespread solution is provided by cement-bentonite mixtures. The construction process is in this case performed in one single phase: a series of alternate panels are excavated, using the cement-bentonite slurry as a stabilizing fluid. The same material is then left in the trench to harden at the end of the excavation (Jefferies, 1971). This construction process not only allows the continuity of the barrier to be easily assured, but it also permits the installation of monitoring and measuring devices in the liquid slurry, avoiding potential damage induced by the perforation of the solid material (Sanetti, 1998, 2000). The goal of these devices is generally to collect the fluid passing through the barrier before the leachate contaminates the surrounding environment, allowing an early identification of contaminants and an assessment of the efficiency of the barrier for monitoring purposes. In this paper, the working principles of a (patented) monitoring device to be installed in self-hardening cement-bentonite cut-off walls are investigated by means of numerical simulations. In Section 2, just the hydraulic response of the barrier is analyzed, while in Section 3 the presence of a dilute contaminant is addressed too.

2 Hydraulic behavior of the barrier

2.1 The numerical model

A scheme of a parallelepiped cut-off wall (panel) with the monitoring devices is shown in Figure 1(a). As a first approximation, the device can be considered as a cylinder that allows the drainage of the pore fluid on the whole lateral surface. The hydraulic head inside the device is supposed to be known, and equal to h_{dev}. By assuming that the vertical component of fluid velocity can be disregarded, a two dimensional scheme can be adopted, as shown in the plan view in Figure 1(b). By assuming the homogeneity of the cement-bentonite mixture, the symmetry of the problem allows studying just a part of the wall, centered in the devices and characterized by a length s. The system can thus be described by just three geometrical variables, namely (i) the thickness t of the barrier, (ii) the diameter d of the device, and (iii) the spacing s between the devices. In the numerical study, some geometrical configurations of the system have been studied, by changing the spacing and the diameter of the devices for a given wall thickness.
In order to study the hydraulic response of the system, just the water flow in the barrier (assumed to be water saturated) is considered, neglecting the presence of contaminants. Assuming that the specific discharge of the porous medium $\mathbf{v}$ and the gradient of the hydraulic head h are linearly related by the Darcy law through the hydraulic conductivity

K_b, the governing equation for an isotropic and homogenous material can be simply expressed by the Laplace equation:

$$\nabla^2 h = 0. \tag{1}$$

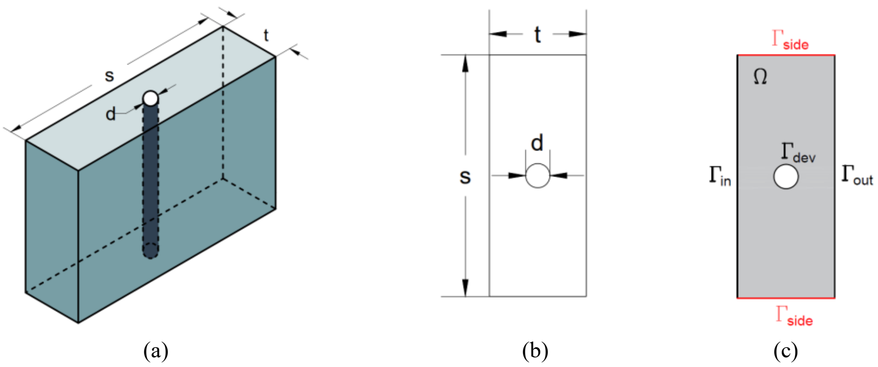

Fig. 1 Geometrical variables (a), plan view (b) and boundary conditions (c)

The boundary conditions for the problem at hand are summarized in Figure 1(c): the hydraulic head $h = h_{in}$ on the inlet surface Γ_{in} (i.e. the part of the wall in contact with the contaminated area) is supposed to be known, as well as the hydraulic head $h = h_{out}$ at the outlet surface Γ_{out}, being $h_{in} > h_{out}$. In all the following numerical analyses, the hydraulic head difference between the sides of the wall is supposed to be constant and equal to 1 m. On the lateral surface of the device Γ_{dev} a constant hydraulic head is imposed too, i.e. $h = h_{dev}$. Finally, due to the symmetry of the fluxes, on the lateral sides of the domain Γ_{side} a no flux condition is imposed. For the sake of making the results of the analyses as general as possible, the model has been formulated in a non-dimensional fashion, according to the following non-dimensional groups: s/t (normalized device spacing), d/t (normalized device diameter), h^* (normalized hydraulic head in the device), defined as $h^* = (h_{dev}-h_{out})/(h_{in}-h_{out})$. In particular, h^* varies from 1 – when the hydraulic head in the device coincides with the inlet hydraulic head h_{in}- to 0 – when $h_{dev} = h_{out}$. Equation (1), together with the relevant boundary conditions, has been numerically solved via the Finite Element Method, by using the software Comsol Multiphysics ®.

2.2 *Numerical results*

In this section, some numerical results are presented, with the aim of evidencing the role of the hydraulic and geometrical variables on the hydraulic response of the system. When the results are not shown in a non-dimensional fashion, reference is made to 0.4 m thickness cut-off wall, made of a cement-bentonite mixture characterized by a hydraulic conductivity $K_b = 10^{-9}$ m/s, as suggested by regulations (ICE, 1999). In every simulation, the flow across the outlet boundary of the wall, q_{out}, has been calculated, as well as the flow of water inside the device, q_{dev}. The following variables have then been defined:

- The equivalent hydraulic conductivity of the cutoff wall with the device, $K_{eq} = q_{out}/s \cdot t/\Delta h$, being $\Delta h = h_{in}-h_{out}$;
- The hydraulic efficiency of the system, expressed in terms of the reduction of the equivalent hydraulic conductivity of the system with respect to the hydraulic conductivity of the cement-bentonite mixture, $Eff = (K_b-K_{eq})/K_b$. It is easy to prove that the efficiency Eff can be expressed also in terms of water flow as $Eff = (q_{Darcy} - q_{out})/q_{Darcy}$, where q_{Darcy} is the water flow that would be obtained without the device.

It is worth noting that, from the hydraulic point of view, a functional system should be characterized by a positive efficiency Eff, i.e. having an outward flow lower than the inward one. As expected, for a negligible size of the device, positive efficiency is guaranteed for $h^* < 0.5$. In order to clarify this aspect, Figure 2(a) shows the calculated values of hydraulic head and the velocity flow lines for a device characterized by $h^* = 0.1$. In this case the efficiency is positive and an inward flow in the device is obtained, thus reducing the flow of water from the outlet surface of the wall. Vice versa, Figure 2(b) shows the numerical results for $h^* = 0.8$. In this case, the efficiency is negative and the flow of water is outward from the device to the wall, thus increasing the quantity of water crossing the outward surface of the wall. In the following, just configurations with positive efficiency will be considered: the presence of the device – at least from the hydraulic point of view – provides a mitigation effects, reducing the flow of water crossing the barrier.

Figure (3) shows a collection of results from several finite analyses performed to evidence the role of device spacing and diameter on the hydraulic efficiency of the system. It is evident that the lower the spacing s and the head in the device h^*, the larger the efficiency. The role of device diameter is instead less straightforward. Figure 3(a) shows that, for $h^*=0$, the efficiency always increases with the increase of the diameter of the device, while for $h^*>0$ the evolution of Eff with d/t is non monotonic. In fact, for large diameters, the hydraulic head difference between the device and the outlet boundary is imposed at a small distance, thus inducing a large hydraulic gradient and an increase in the magnitude of the outward flow from the device.

To provide a tool that can be useful for the identification of the optimal configuration of the system from the hydraulic point of view, the diameters corresponding to the maximum efficiency are collected in Fig. 4 for different spacings and hydraulic heads in the device. Next to each point, the corresponding efficiency is reported.

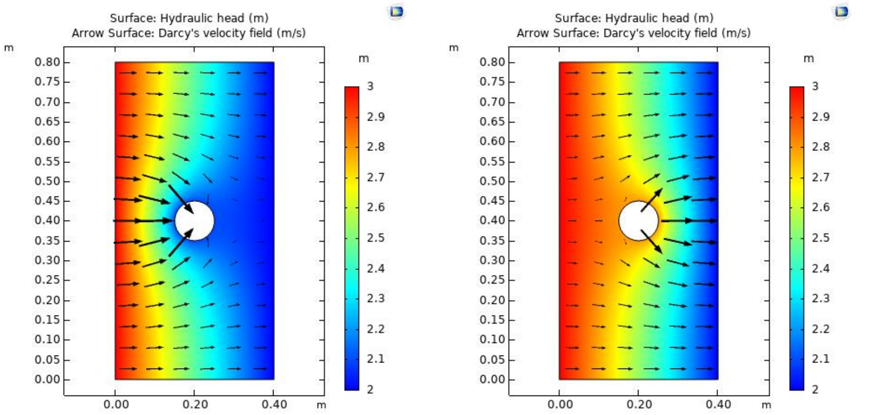

(a) h* = 0.1 (b) h* = 0.8

Fig. 2 Role of the hydraulic head in the device h* on the hydraulic head distribution and on fluid velocity flow lines.

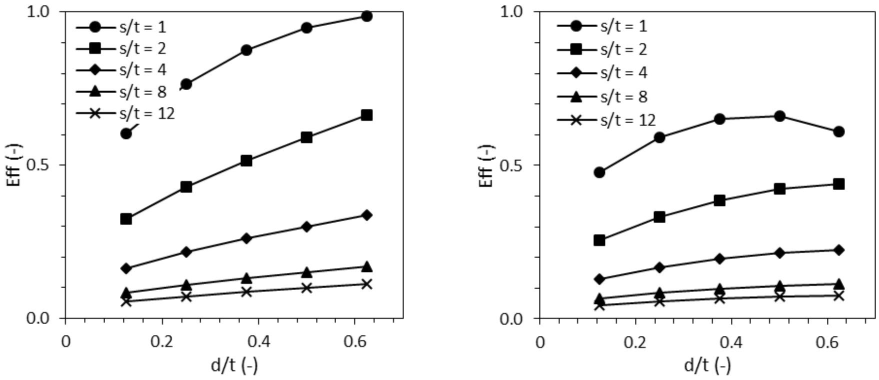

(a) h* = 0.0 (b) h* = 0.1

Fig. 3 Evolution of hydraulic efficiency of the system with device diameter for different spacings.

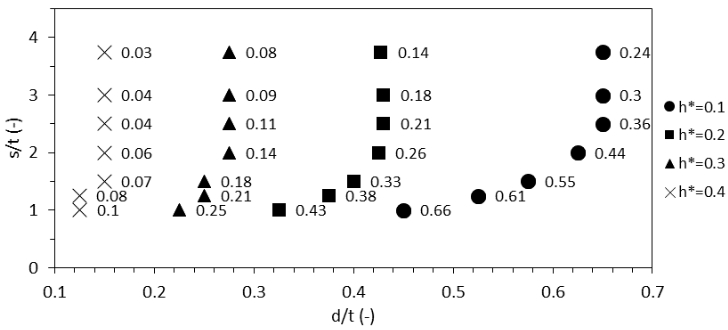

Fig. 4. Optimal geometrical configuration for different h^* values and related hydraulic efficiency.

3 Solute transport in the barrier: numerical model

3.1 The numerical model

As discussed in the introduction, slurry trench cut-off walls are widely used also for the containment of subsurface pollution. The requirement for the backfill material to have a hydraulic conductivity K_b lower than 10^{-9} m/s is in fact specified in slurry wall design because, under such condition, contaminant diffusion can be reasonably assumed to be the relevant transport process (Devlin & Parker, 1996). In the design of slurry walls, the determination of either the potential service life (which is usually related to the break-through time of the contaminant) for a given wall thickness or the wall thickness required for a target service life is generally performed considering the contaminant flux as a one-dimensional advective-dispersive process, see e.g. Li et al (2017). The presence of the monitoring device however might have a relevant effect on the specific discharge direction, as proved in the previous sections, making the one-dimensional assumption not reliable to properly describe the advection process. Neglecting porosity changes, the two-dimensional contaminant mass balance equation for a diluted contaminant is thus considered:

$$R\phi \frac{\partial c}{\partial t} + \nabla \cdot \boldsymbol{j} = 0, \tag{2}$$

where c is the molar contaminant concentration, R is the retardation factor, ϕ is porosity and $\mathbf{j}$ the contaminant flux. The transport of the solute can be expressed as the sum of two contributions, namely advection and dispersion. Dispersion accounts for the direct flow of the contaminant mass, and thus, is related to chemical concentration gradients, while advection represents the movement of the contaminant mass due to the flowing water. Accordingly, the total contaminant flux reads:

$$\boldsymbol{j} = c\mathbf{v} - D\nabla c, \tag{3}$$

being D the effective dispersion parameter of the cement-bentonite mixture, accounting for molecular diffusion, porosity and tortuosity (see, e.g., Della Vecchia & Musso, 2016). The system of equation (1) and (2) is thus solved numerically by means of the Finite Element Method, again using the software Comsol Multiphysics ®. The initial and boundary conditions imposed to solve equation (2) are:

- Initial condition: the backfill is assumed to be free of contaminant everywhere: $c(\mathbf{x}, t = 0)=0$ on Ω;
- Inlet boundary Γ_{in}: according to van Genuchten & Parker (1994), a Robin boundary condition is applied, guaranteeing a constant flux through the inlet boundary and mass balance consistency :

  $$(c\mathbf{v} - D\nabla c) \cdot \mathbf{n} = (\, c_{in}\mathbf{v}) \cdot \mathbf{n}, \tag{4}$$

  being c_{in} the inlet concentration and $\mathbf{n}$ the normal unit vector to the boundary;
- Outlet boundary Γ_{out}: $(\nabla c) \cdot \mathbf{n} = 0$, in order to achieve a constant concentration gradient across the outlet boundary, according to Prince et al (2000).

- Device lateral surface Γ_{dev}: $c = 0$, due to the continuous removal of water from the device in order to keep the hydraulic head constant.

3.2 Numerical results

Some preliminary simulations of contaminant propagation through the cutoff wall without the device have been run ($\Delta h = 1$ m, $h^* = 0$, $D = 2.5 \cdot 10^{-12}$ m^2/s). Figure 5 shows the breakthrough curves for the contaminant in terms of the evolution of the average normalized concentration on Γ_{out} c_{out}/c_{in} with the non-dimensional time T. The non-dimensional time has been defined as $T = tv/D$, being v the water velocity in the 1D case (i.e. when no devices are present) and t the time. It is evident that, for hydraulic conductivities larger than 10^{-11} m/s, the slope of the breakthrough curve increases with K_b. Vice versa, for K_b values lower than 10^{-11} m/s, the breakthrough curve is insensitive to K_b. This effect can be related to a well-known non-dimensional variable, the Péclet number, which in this case is defined as:

$$Pe = \frac{vL}{D}, \tag{5}$$

where L is the length of the one-dimensional path, in this case coincident with the thickness of the cutoff wall. This number is a measure of the relative importance of advection to dispersion. For the considered material parameters and geometrical configuration, $K_b = 10^{-11}$ m/s leads to $Pe = 0.04$: such a low Péclet number implies a negligible contribution of advection with respect to diffusion, so that the response of the system does not depend anymore on the hydraulic conductivity of the backfill, but just on its dispersion coefficient (which is the same in all the simulations). The role of the geometrical configuration of the devices on contaminant propagation through the barrier is evidenced in Fig. 6, which shows the breakthrough curves on Γ_{out} for the cutoff wall without devices, as well as for device spacing $s/t = 1$, 2 and 4. Numerical results in Fig. 6 have been obtained by setting the hydraulic conductivity $K_b = 10^{-9}$ m/s.

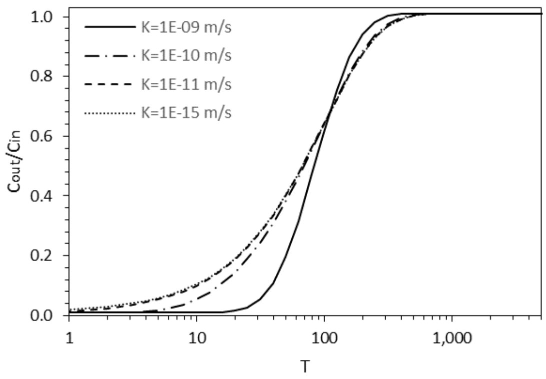

Fig. 5 Influence of the backfill hydraulic conductivity on the outlet breakthrough curves for the cutoff wall without devices.

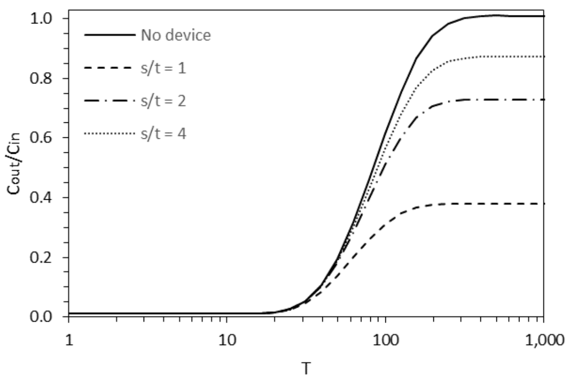

Fig. 6 Influence of the geometry of the barrier (*s/t*) on the breakthrough curves for $K_b = 10^{-9}$ m/s.

The mitigation role of the device is evident: at the same time, the lower the spacing between devices, the lower the concentration at the outlet boundary. The effect is more evident when stationary conditions are approached. The reduction of the concentration at the outlet is related to a larger contaminant mass removal through the devices, which is triggered by the zero-concentration condition imposed on their walls. The division of contaminant fluxes (normalized with respect to the inlet flux) between the outlet boundary and the device for s/t = 1 are shown in Figure 7: more than 90% of contaminant mass is removed by the device. However, it is well known that the hydraulic conductivities determined by in situ testing are larger than those found from laboratory measurements, as a consequence of the heterogeneity in the constructed wall and of the effects of large-scale testing, where inclusions and fissures may form a network of flow paths. Accordingly, numerical simulations conducted considering a larger hydraulic conductivity, $K_b = 10^{-8}$ m/s, and the same dispersion coefficient are shown in Fig. 8. In this case, the larger seepage velocity (i.e. the larger Péclet number) reduces the role of diffusion with respect to advection and makes the breakthrough curve less dependent on device spacing. Furthermore, the effect of the devices is primarily to retard the arrival at the outlet of the contaminant, rather than to reduce the outlet concentration at steady state conditions.

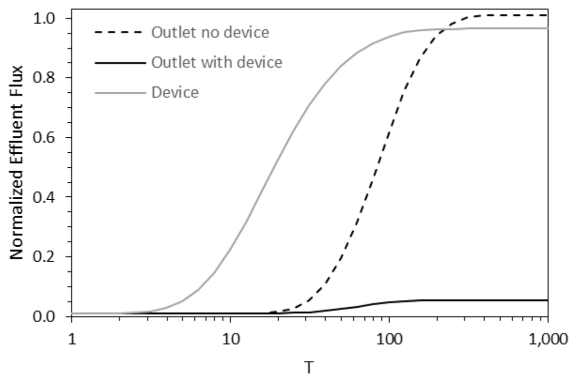

Fig. 7 Subdivision of normalized fluxes (continuous line) between the device and the outlet boundary for s/t =1, compared with the flux (dashed line) at the outlet boundary when no devices are present.

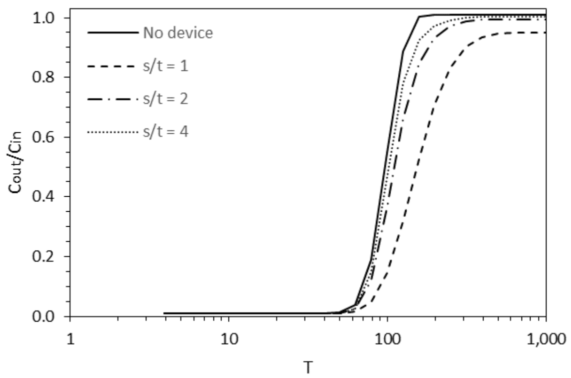

Fig. 8 Influence of the geometry of the barrier (s/t) on the breakthrough curves for $K_b = 10^{-8}$ m/s.

4 Conclusions

In the present study, some numerical analyses have been performed to evaluate the performance of slurry trench cutoff walls with a device embedded for monitoring purposes. In the first part of the paper, the hydraulic response of the system has been studied, identifying the role of the main geometric variables of the wall and of the device. In particular, the role of device diameter, spacing and hydraulic head have been identified in terms of non-dimensional variables, leading to a rational criterion to identify the configuration of the system corresponding to the maximum hydraulic efficiency in terms of reduction of water flow from the cutoff wall. In the second part of the paper, transport across the barrier of a diluted contaminant has been considered too. In this case, the role of another non-dimensional variable has been put in evidence, i.e. the Péclet number. For low Péclet numbers, the transport of the contaminant is dominated by dispersion/diffusion mechanisms, while for larger Péclet numbers advection begins to play a relevant role. The consequences on the behavior of cutoff walls are put in evidence, with particular reference to the role played by the devices and their geometry. Further studies will focus on the effect of contaminant concentration on material transport properties.

Acknowledgements The activity presented in the paper is part of the public administration agreement between Politecnico di Milano -Department of Civil and Environmental Engineering and the Italian Ministry of Economic Development, Direzione Generale per la Sicurezza anche Ambientale delle Attività Minerarie ed Energetiche – Ufficio Nazionale Minerario per gli Idrocarburi e le Georisorse – Programme Clypea.

References

Della Vecchia, G. and Musso, G. (2016). Some remarks on single and double porosity modelling of coupled chemo-hydro-mechanical processes in clays. *Soils and Foundations* 56 (5), 779-789.

Devlin, J. F., and Parker, B. L. (1996). Optimum hydraulic conductivity to limit contaminant flux through cutoff walls. *Groundwater* 34(4), 719-726.

ICE (1999). Specification for the construction of slurry trench cut-off walls as barriers to pollution migration. Thomas Telford.

Joshi, K., Kechavarzi, C., Sutherland, K., Ng, M. Y. A., Soga, K., and Tedd, P. (2010). Laboratory and in situ tests for long-term hydraulic conductivity of a cement-bentonite cutoff wall. *Journal of Geotechnical and Geoenvironmental Engineering* 136(4), 562-572.

Li, Y. C., Chen, G. N., Chen, Y. M., and Cleall, P. J. (2017). Design Charts for Contaminant Transport through Slurry Trench Cutoff Walls. *Journal of Environmental Engineering* 143(9), 06017005.

Prince, M. J., Maneval, J. E., and Evans, J. C. (2000). Analysis of boundary conditions for contaminant transport through adsorptive, low-permeability slurry trench cutoff walls. *Environmental Geotechnics*, 58-72.

Sanetti, G. (1998). Diaframmi plastici a base di cemento bentonite. *Quarry and Construction*, novembre 1998, 51-55.

Sanetti G. (2000). Diaframmi plastici: evoluzione e nuovi sistemi di controllo post-operam. *Quarry and Construction*, dicembre 2000, 105-109.

Soga, K, Joshi, K and Evans, J.C. (2013). Cement bentonite cutoff walls for polluted sites. *Coupled Phenomena in Environmental Geotechnics* – Manassero et al (Eds), Taylor and Francis Group, London, 149-165.

Van Genuchten, M. T., and Parker, J. C. (1984). Boundary Conditions for Displacement Experiments through Short Laboratory Soil Columns 1. *Soil Science Society of America Journal* 48(4), 703-708.